Proceedings of the International Association for Shell and Spatial Structures (IASS) Symposium 2010, Shanghai
Spatial Structures – Permanent and Temporary
November 8-12 2010, Shanghai, China

Ice Pantheon Project 2010

Takaya Suzuki[1)], Tsutomu Kokawa[2)], Koji Watanabe[3)]

[1)] Engineer, Taisei Corporation, [2)] Professor, [3)] Assoc. Prof., School of Design, Tokai University
Kamuicho Chuwa 224, Asahikawa, Japan
kokawa@tspirit.tokai-u.jp

Abstract

According to the shape and the creep deflection analysis of an axisymmetric ice dome, a non-spherical ice dome improves significantly the structural performance compared to the conventional type of spherical dome. The analysis of an axisymmetric ice dome is based on the followings: membrane theory for a thin shell and invariant theory for the ice obeyed Glen's law during the secondary creep stage. In addition to the numerical results of the analysis, the past construction experiences and the field experiments of 20-30m span ice domes would support the realization of a huge ice dome spanning 40 meters never existed before, which has almost same size as Pantheon in Rome well known as one of the biggest classical stone dome. The ice dome is easier to construct than the stone dome and the strength/density of the ice is almost same as that of stone in short term loading, so it could be possible for students as amateur to construct a 40m-span ice dome if they gradually experience the construction from small domes. Towards the realization of the ice dome, so called 'Ice Pantheon', the students started to go on an exciting, thrilling and wonderful voyage under the technical guidance by the authors. In winter of 2009, as the first step toward this end, a small size of 10-m span ice dome was constructed. And then, in this winter of 2010, a non-spherical 15-m span ice dome was constructed by them and used as event architecture.

Keywords: non-spherical ice dome, shape and creep deflection analysis, Ice Pantheon, student self-built

1 Introduction

Ice shells, which are thin curved plate-structures made of ice, are being used as winter structures in inland Hokkaido with sufficient snow and low temperature [1]. As the typical example of the applications, since 1997 in Tomamu, many ice shells are being used each winter for about 3 months as leisure-recreational facilities after skiing. The shell creates a beautiful space in the environment from the translucent thin plate and the unique curved surface shape. The interior space has a translucent atmosphere with full of natural light in daytime, and the exterior looks like a gigantic illuminator in the dark at night. The shell has also high structural efficiency, because the shape determined from the reticular geometry of the covered ropes on a pneumatic membrane follows automatically so that it works mainly compressive stress under self-weight load. Furthermore, the construction method of blowing snow and spraying water onto the pneumatic formwork has constructional rationality. Through these advantages, it is recognized that the ice shell is a practical ice structure for winter activities in inland Hokkaido. Although the span of the shell for actual use has always been limited to 15-meters or less so far, the application of a 20~30 m span ice dome to an architectural facility would be practicable based upon the field experiments of large ice domes[5][6].
According to the shape and the creep deflection analysis of an axisymmetric ice dome, a non-spherical ice dome improves significantly the structural performance compared to the conventional type of spherical dome. The analysis of a non-spherical ice dome is based on the followings: membrane theory for a thin shell and invariant theory for the ice obeyed Glen's law during the secondary creep stage [2][3][4]. In addition to the numerical result of the analysis, the past construction experiences and field experiments of 20-30m span ice domes [5][6] would support the

realization of a huge ice dome spanning 40 meters never existed before, which has almost same size as Pantheon in Rome well known as one of the biggest classical stone dome. The ice dome is easier to construct than stone dome and the strength/density of the ice is almost same as that of stone in short term loading, so it could be possible for students as amateur to construct a 40m-span ice dome if they gradually experience the construction from small domes. Towards the realization of the ice dome, so called 'Ice Pantheon', the students started to go on an exciting, thrilling and wonderful voyage under the technical guidance by the authors. In winter of 2009, as the first step toward this end, a small size of 10-m span ice dome was constructed. And then, in this winter of 2010, the students constructed a non-spherical 15-m span ice dome. After that, the students also designed and produced the internal and external space of the dome. And they carried out the events by organizing student events.

2 Theoretical consideration on shape and creep deflection

So far, a spherical cap is often used as the shape of ice dome. However, in the case of a large span such as Ice Pantheon, a large creep deformation may occur under gravity load. The large deformation is not good for the structural stability. "Form follows force" as one says, and a non-spherical shape might be able to reduce the amount of creep deformation. That might enhances the structural performance of the ice dome.

2.1 Shape analysis

The shape analysis of a non-spherical ice dome is based on membrane theory for a thin shell [2]. Let us consider a dome of nonuniform thickness supporting its own weight. Fig.1 shows an element of a dome that is cut by two adjacent meridians and two parallel circles. The weight of the dome per unit area of the middle surface is ρh, and the two components of this weight along the coordinate axes are

$$p_\varphi = \rho h \sin\varphi \qquad p_n = \rho h \cos\varphi \qquad (1)$$

Where ρ is the density of ice and h is the ice thickness. The equation of equilibrium in the radial direction is

$$\frac{N_\varphi}{r_1} + \frac{N_\theta}{r_2} = -p_n \qquad (2)$$

Where N_φ, N_g are the magnitudes of the membrane forces per unit length as shown in the Fig. 1. Let's assume that N_φ, N_θ are given in advance by Eq. (3).

$$N_\varphi = -\sigma_o h f_\varphi(\varphi), \qquad N_\theta = -\sigma_o h f_\theta(\varphi) \qquad (3)$$

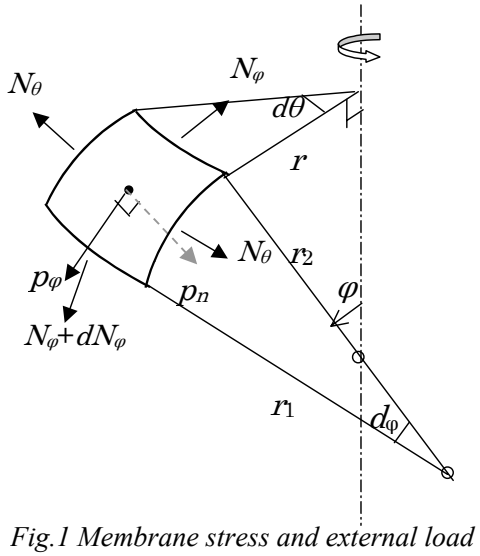

Fig.1 Membrane stress and external load

Where σ_o is the compressive stress at the apex of the dome, and f_φ, f_θ are the distribution function of the membrane forces along the coordinate axes. f_φ, f_θ are functions of φ and 1 for φ=0. Substituting Eq. (1) and (3) into Eq.(2),

$$\sigma_o h\left(\frac{f_\varphi}{r_1} + \frac{f_\theta}{r_2}\right) = \rho h \cos\varphi \qquad (4)$$

Using Eq. (4), $r = r_2 \sin\varphi$ *and* $r_1 d\varphi = \dfrac{dr}{\cos\varphi}$ as shown in Fig.1, Eq.(5) forms a first order of differential equation for β.

$$\frac{d\beta}{d\varphi}=\frac{\beta f_\varphi\cos\varphi}{\beta\cos\varphi-f_\theta\sin\varphi},\quad where\quad \beta=\alpha r,\quad \alpha=\frac{\rho}{\sigma_o} \tag{5}$$

Under the initial condition that $\frac{d\beta}{d\varphi}=2$ *for* $\varphi\to 0,$ the numerical solution of Eq. (5) can be calculated by applying Runge-Kutta Method. Using the numerical value of β, z and r of the dome' shape are computed numerically based on Eq. (6)

$$\therefore \alpha(z-z_o)=\lim_{\varphi_o\to 0}\int_{\varphi_o}^{\varphi}\frac{\beta f_\varphi\sin\varphi}{\beta\cos\varphi-f_\theta\sin\varphi}d\varphi,\qquad \alpha r=\beta \tag{6}$$

Next, the thickness of the ice h is derived as follows. The equation of the equilibrium in the meridian direction is

$$\frac{d(N_\varphi r)}{d\varphi}-N_\theta r_1\cos\varphi+p_\varphi r_1 r=0 \tag{7}$$

Substituting $N_\varphi=-\sigma_o h f_\varphi,\quad N_\theta=-\sigma_o h f_\theta\quad and\quad p_\varphi=\rho h\sin\varphi$ into Eq. (7), Eq. (8) is obtained.

$$\frac{1}{Q}\frac{dQ}{d\varphi}=\frac{(f_\theta-f_\varphi)\cos\varphi+\beta\sin\varphi}{\beta\cos\varphi-f_\theta\sin\varphi},\qquad where\quad Q=hf_\varphi \tag{8}$$

Solving Eq. (8) and placing $Q=Q_o\,(=h_o)$ for $\varphi=\varphi_o\to 0$, h becomes Eq. (9).

$$\therefore\left(\frac{h}{h_o}\right)=\left(\frac{1}{f_\varphi}\right)\exp\left(\lim_{\varphi_0\to 0}\int_{\varphi_0}^{\varphi}\left(\frac{\beta\sin\varphi+(f_\theta-f_\varphi)\cos\varphi}{\beta\cos\varphi-f_\theta\sin\varphi}\right)d\varphi\right) \tag{9}$$

Where h_o is the thickness at the apex of the dome.

2.2 Creep deflection

The creep model for the ice is assumed to be obeyed Glen's law during the secondary creep [3].

$$\frac{d\varepsilon}{dt}=\dot{\varepsilon}=k\sigma^n \tag{10}$$

Where σ is uniaxial stress, $\dot{\varepsilon}$ is uniaxial strain rate and k, n is constant.
Strain-displacement relation is shown in Eq. (11).

$$\varepsilon_\theta=\frac{v\cos\varphi-w\sin\varphi}{r}=\frac{v\cot\varphi-w}{r_2}$$
$$\varepsilon_\varphi=\frac{v'-w}{r_1} \tag{11}$$

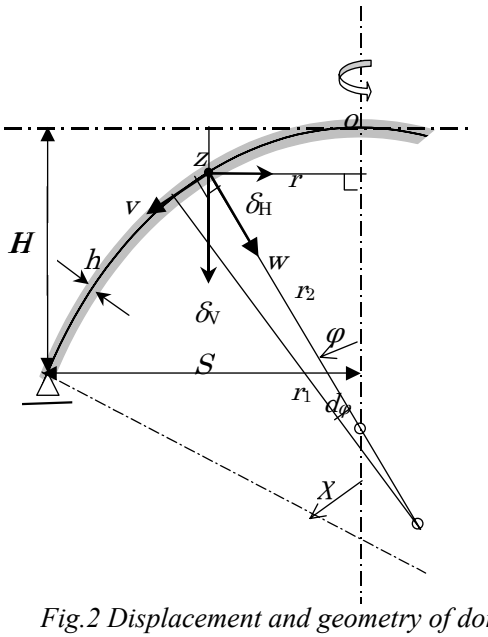

Fig.2 Displacement and geometry of dome

Where $' = \frac{d}{d\varphi}$, w is the displacement in the radial direction, v is the displacement in the meridian direction, as shown Fig.2, ε_θ is strain in the parallel direction and ε_φ is strain in the meridian direction. The relationship between the strain rate and the membrane stress is written in Eq. (12) by applying invariant theory [4].

$$\dot{\varepsilon}_\varphi = k\left(\sigma_\varphi - \frac{1}{2}\sigma_\theta\right)\left(\sigma_\varphi{}^2 - \sigma_\varphi\sigma_\theta + \sigma_\theta{}^2\right)^{\frac{n-1}{2}} = -k\sigma_o{}^n\left(f_\varphi - \frac{1}{2}f_\theta\right)\left(f_\varphi{}^2 - f_\varphi f_\theta + f_\theta{}^2\right)^{\frac{n-1}{2}}$$
$$\dot{\varepsilon}_\theta = -k\sigma_o{}^n\left(f_\theta - \frac{1}{2}f_\varphi\right)\left(f_\varphi{}^2 - f_\varphi f_\theta + f_\theta{}^2\right)^{\frac{n-1}{2}}, \text{where} \quad \sigma_\varphi = \frac{N_\varphi}{h} = \sigma_o f_\varphi, \quad \sigma_\theta = \frac{N_\theta}{h} = \sigma_o f_\theta \tag{12}$$

Eliminating w in Eq. (11) and using Eq. (12), Eq. (13) forms the first order of ordinary differential equation for $\dot{v}$.

$$\dot{v}' - \dot{v}\cot\varphi = r_1\dot{\varepsilon}_\varphi - r_2\dot{\varepsilon}_\theta = F(\varphi)$$
$$\text{where} \quad F(\varphi) = r_1\dot{\varepsilon}_\varphi - r_2\dot{\varepsilon}_\theta = k\sigma_o{}^n r\left(f_\varphi{}^2 - f_\varphi f_\theta + f_\theta{}^2\right)^{\frac{n-1}{2}}\left\{-\frac{f_\varphi\left(f_\varphi - \frac{1}{2}f_\theta\right)}{\beta\cos\varphi - f_\theta\sin\varphi} + \frac{\left(f_\theta - \frac{1}{2}f_\varphi\right)}{\sin\varphi}\right\} \tag{13}$$

The general solution of Eq.(13) is $\dot{v} = \sin\varphi\left\{\int_0^\varphi \frac{F(\varphi)}{\sin\varphi}d\varphi + C\right\}$ (14)

Where C is a constant of integration to be determined from the condition at the support. Using the $\dot{v}$ in Eq. (14), $\dot{w}$ is written in Eq. (15)

$$\dot{w} = \dot{v}\cot\varphi - r_2\dot{\varepsilon}_\theta = \cos\varphi\left\{\int_0^\varphi \frac{F(\varphi)}{\sin\varphi}d\varphi + C\right\} + r_2 k\sigma_o{}^n\left(f_\theta - \frac{1}{2}f_\varphi\right)\left(f_\varphi{}^2 - f_\varphi f_\theta + f_\theta{}^2\right)^{\frac{n-1}{2}} \tag{15}$$

The vertical displacement rate $\dot{\delta}_V$ shown in Fig. 2, is expressed by Eq. (16).

$$\dot{\delta}_V = \dot{v}\sin\varphi + \dot{w}\cos\varphi \tag{16}$$

The constant C is determined from the condition that for $\varphi=\chi$,, the vertical displacement rate $\dot{\delta}_v$ is zero.

$$\therefore C = -\int_0^\chi \frac{F(\varphi)}{\sin\varphi}d\varphi - \bar{r}_2 k\sigma_o{}^n\left(\bar{f}_\theta - \frac{1}{2}\bar{f}_\varphi\right)\left(\bar{f}_\varphi{}^2 - \bar{f}_\varphi\bar{f}_\theta + \bar{f}_\theta{}^2\right)^{\frac{n-1}{2}}\cos\chi \tag{17}$$

Where $\overline{\nabla}$ is ∇ for $\varphi=\chi$.

Therefore, $\dot{\delta}_v$ and the horizontal displacement rate $\dot{\delta}_H = -\dot{v}\cos\varphi + \dot{w}\sin\varphi$ are written as follows.

$$\dot{\delta}_H = -\dot{v}\cos\varphi + \dot{w}\sin\varphi = r_2 k\sigma_o{}^n\left(f_\theta - \frac{1}{2}f_\varphi\right)\left(f_\varphi{}^2 - f_\varphi f_\theta + f_\theta{}^2\right)^{\frac{n-1}{2}}\sin\varphi$$
$$\dot{\delta}_V = \dot{v}\sin\varphi + \dot{w}\cos\varphi \tag{18}$$
$$= -\int_\varphi^\chi \frac{F(\varphi)}{\sin\varphi}d\varphi + k\sigma_o{}^n\left\{r_2\left(f_\theta - \frac{1}{2}f_\varphi\right)\left(f_\varphi{}^2 - f_\varphi f_\theta + f_\theta{}^2\right)^{\frac{n-1}{2}}\cos\varphi - \bar{r}_2\left(\bar{f}_\theta - \frac{1}{2}\bar{f}_\varphi\right)\left(\bar{f}_\varphi{}^2 - \bar{f}_\varphi\bar{f}_\theta + \bar{f}_\theta{}^2\right)^{\frac{n-1}{2}}\cos\chi\right\}$$

And then substituting

$$\beta=\alpha r,\quad \alpha=\frac{\rho}{\sigma_o},\qquad F(\varphi)=r_1\dot{\varepsilon}_\varphi-r_2\dot{\varepsilon}_\theta=rk\sigma_o{}^n\left(f_\varphi{}^2-f_\varphi f_\theta+f_\theta{}^2\right)^{\frac{n-1}{2}}\left\{-\frac{f_\varphi\left(f_\varphi-\frac{1}{2}f_\theta\right)}{\beta\cos\varphi-f_\theta\sin\varphi}+\frac{\left(f_\theta-\frac{1}{2}f_\varphi\right)}{\sin\varphi}\right\}$$

$$and\quad E(\varphi)=\frac{\alpha}{k\sigma_o{}^n}\frac{F(\varphi)}{\sin\varphi}=\beta\left(f_\varphi{}^2-f_\varphi f_\theta+f_\theta{}^2\right)^{\frac{n-1}{2}}\left\{-\frac{f_\varphi\left(f_\varphi-\frac{1}{2}f_\theta\right)}{\sin\varphi(\beta\cos\varphi-f_\theta\sin\varphi)}+\frac{\left(f_\theta-\frac{1}{2}f_\varphi\right)}{\sin^2\varphi}\right\}$$

into Eq.(18), $\dot{\delta}_H$ and $\dot{\delta}_v$ are written in Eq. (19).

$$\begin{aligned}&\therefore\alpha\dot{\delta}_H=k\sigma_o{}^n\beta\left(f_\theta-\frac{1}{2}f_\varphi\right)\left(f_\varphi{}^2-f_\varphi f_\theta+f_\theta{}^2\right)^{\frac{n-1}{2}}\\&\therefore\alpha\dot{\delta}_V=k\sigma_o{}^n\left[\left\{\frac{\beta}{\sin\varphi}\left(f_\theta-\frac{1}{2}f_\varphi\right)\left(f_\varphi{}^2-f_\varphi f_\theta+f_\theta{}^2\right)^{\frac{n-1}{2}}\cos\varphi-\frac{\overline{\beta}}{\sin\chi}\left(\bar{f}_\theta-\frac{1}{2}\bar{f}_\varphi\right)\left(\bar{f}_\varphi{}^2-\bar{f}_\varphi\bar{f}_\theta+\bar{f}_\theta{}^2\right)^{\frac{n-1}{2}}\cos\chi\right\}-\int_\varphi^\chi E(\varphi)d\varphi\right]\end{aligned}\qquad(19)$$

The displacement rate at the apex $\dot{\delta}_{Vtop}$ is

$$\therefore\alpha\dot{\delta}_{V\,top}=k\sigma_o{}^n\left\{1-\overline{\beta}\left(\bar{f}_\theta-\frac{1}{2}\bar{f}_\varphi\right)\left(\bar{f}_\varphi{}^2-\bar{f}_\varphi\bar{f}_\theta+\bar{f}_\theta{}^2\right)^{\frac{n-1}{2}}\frac{\cos\chi}{\sin\chi}-\int_0^\chi E(\varphi)d\varphi\right\}\qquad(20)$$

The average vertical displacement rate $\dot{\delta}_{Vav}$ is

$$\dot{\delta}_{V\,av}=\frac{\int_0^\chi\dot{\delta}_V\left(2\pi r r_1 d\varphi\right)}{\int_0^\chi 2\pi r r_1 d\varphi}=\frac{\int_0^\chi\dot{\delta}_V r r_1 d\varphi}{\int_0^\chi r r_1 d\varphi}\qquad(21)$$

2.3 Numerical results for Ice Pantheon Dome

The stress distribution of the membrane forces is given in the following.

$$f_\varphi=\frac{2}{1+\cos(x\chi)},f_\theta=2\left(\cos(x\chi)-\frac{1}{1+\cos(x\chi)}\right),$$

$$Where\quad x=\frac{\varphi}{\chi},\chi=63.435^o$$

The numerical results show a spherical dome of uniform thickness, called S dome. In the case of Ice pantheon dome (IP dome), the following stress distributions are adopted under the condition of the same rise/(base diameter) as the above mentioned S dome.

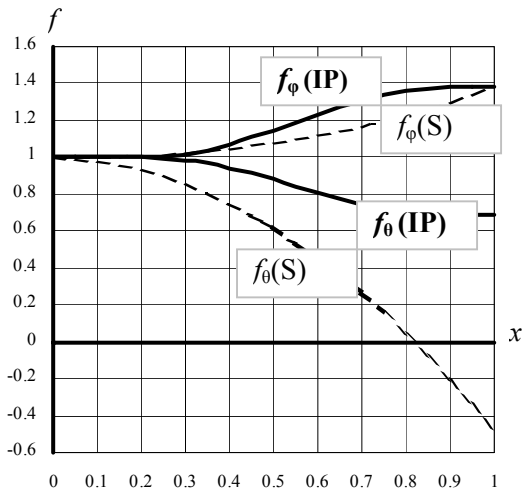

Fig. 3 Distribution of membrane stress

$$\varepsilon_\theta=0\quad for\quad \varphi=\chi,\quad \therefore f_\theta-\frac{1}{2}f_\varphi=0\quad for\quad \varphi=\chi(=55.502^o),\quad x=\frac{\varphi}{\chi}$$

$$f_\varphi=\left\{\begin{array}{cc}1, & 0<x<x_o\\ 1+\frac{k_f}{2}\left(1+\sin\left(\frac{\left(x-0.5(x_1+x_o)\right)\pi}{(x_1-x_o)}\right)\right), & x_o<x<x_1\\ 1+k_f, & x_1<x<1\end{array}\right\},\qquad x_o=0.2,x_1=0.9,$$

$$k_f=2\alpha-1=2\times0.69098\ -1=0.38196\ ,\alpha=\frac{1}{1+\cos\ 63.435^o}=0.69098$$

$$k_t = \frac{(1-k_f)}{2} = \frac{(1-0.38196)}{2} = 0.30902, \qquad f_t = \begin{Bmatrix} 1, & 0 < x < x_o \\ 1 - \frac{k_t}{2}\left(1 + \sin\left(\frac{(x - 0.5(x_1 + x_o))\pi}{(x_1 - x_o)}\right)\right), & x_o < x < x_1 \\ 1 - k_f, & x_1 < x < 1 \end{Bmatrix}$$

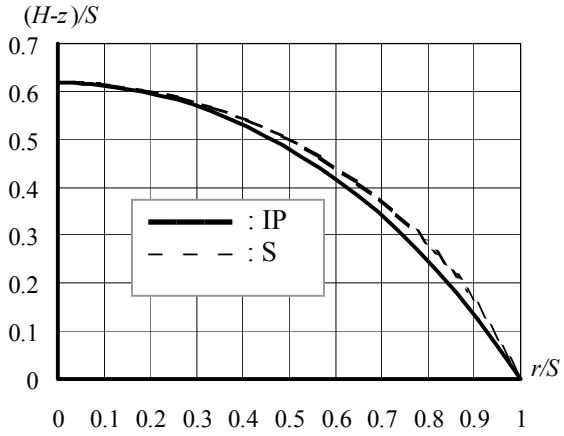

Fig. 4 Meridian curve of dome

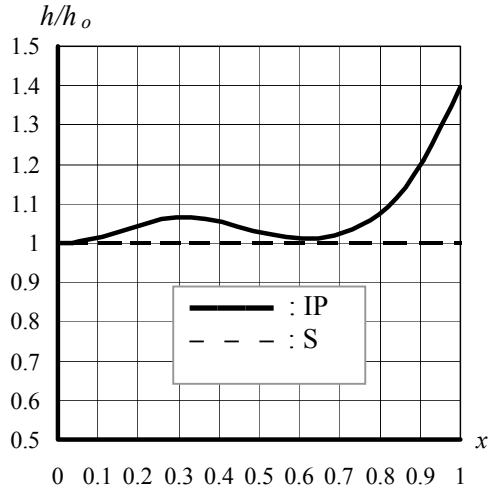

Fig. 5 Distribution of thickness

Fig. 4 and Fig. 5 show the numerical results of these shape analysis. In addition, the creep displacement of IP dome is very small compared to that of S dome as shown in Table 1. From these results, IP dome improves significantly the structural performance such as creep deflection and magnitude of stress compared to S dome. In the case of IP dome spanning 40 m, σ_{OIP} is 7.5 N/cm^2 under its own weight using β = 2.123, ρ=0.85 g/cm^3 and r=20 m in Eq. (5). The value of the σ_{OIP} corresponds to about 1/50th of the uniaxial compressive strength of ice. Therefore, the construction of IP dome spanning 40m has enough strength to stand theoretically.

Table 1 Comparisons of displacement rate and stress between S and IP dome

n (see Eq.(10))	$(\delta_{VIP}/\delta_{VS})_{average}$	$(\delta_{VIP}/\delta_{VS})_{apex}$	$(\sigma_{OIP}/\sigma_{OS})$
1	0.388	0.463	0.842
2	0.263	0.344	
3	0.172	0.244	

δ_{VIP}: vertical displacement rate of IP dome, $\delta_{VS:}$ vertical displacement rate of S dome
$(\delta_{VIP}/\delta_{VS})_{average}$: Ratio of average δ_{VIP} to average $\delta_{VS,}$ $(\delta_{VIP}/\delta_{VS})_{apex}$: Ratio of δ_{VIP} at apex to δ_{VS} at apex
σ_{OIP}: σ_O in IP dome, σ_{OS}: σ_O in S dome

3 Construction of 15 m ice dome

3.1 Outline of constructional sequence

1. Construct snow-ice foundation ring with about a 12.8 m inner diameter.
2. Building up the 3-dimensional formwork by inflating a 2-dimensional membrane bag of 15m diameter, covered with ropes with a reticular pattern (Fig. 6) determined by the geodesic division of the non-spherical shape anchored to the snow-ice foundation ring.
3. Covering the membrane with thin snow-ice sherbet by blowing snow with a rotary snow blower and spraying tap water with an adjustable nozzle. The thin layer snow-ice sherbet is frozen by cold outside air per one operation of snow blowing.
4. Repeat the application of snow and water up to the designed ice thickness (Fig. 7) based on the numerical result in Fig. 5. Then remove the bag and ropes for reuse.

3.2 Geometry of cover rope

Fig. 6 shows the configuration of the cover rope. The reticular pattern is determined by projecting the geodesic pattern of Triacon division 4 frequencies on the spherical part surface with same rise-span ratio to IP surface shown in Fig. 4. Fig. 6 also shows the distances between nodal points. Fig. 7 shows the designed ice thickness based on the Fig.5.

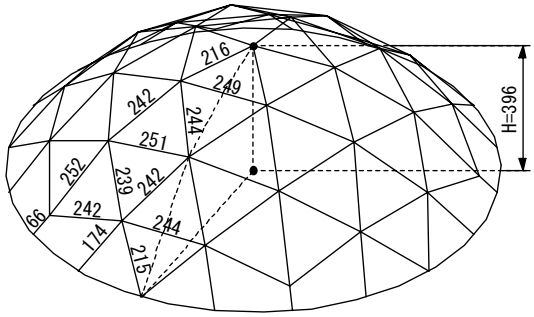

Fig. 6 Reticular pattern and rope length (cm)

3.3 Manufacturing cover rope

The net was made of Φ12 mm polypropylene rope. 'Satuma-Ami' technique was used for manufacturing the rope end that is very strong against the tension force. Supposing maximum water head of the air blower for the inflation as 50 mm Aq., the tension force becomes about 4 KN on computation, so the Φ12 mm P.P. rope is strong enough against 20.6 KN of its breaking tension force. Fig.8 shows the situation of manufacturing the cover rope by students.

3.4 Snow-ice foundation ring

Φ14 mm polypropylen anchor ropes were lashed to interbedded with the snow-ice foundation ring whose inner diameter has about 12.8 m and the section is about 100cm(width)*70cm(height). The ring was constructed by pouring snow and water, and treading down so as to harden and freeze the snow-ice sherbet promptly by students' power without machines as shown in Fig. 9. The weight of the ring is heavy enough against the lifting force under the inflation of pneumatic formwork. The construction work took about 7 hours in days of December 2009.

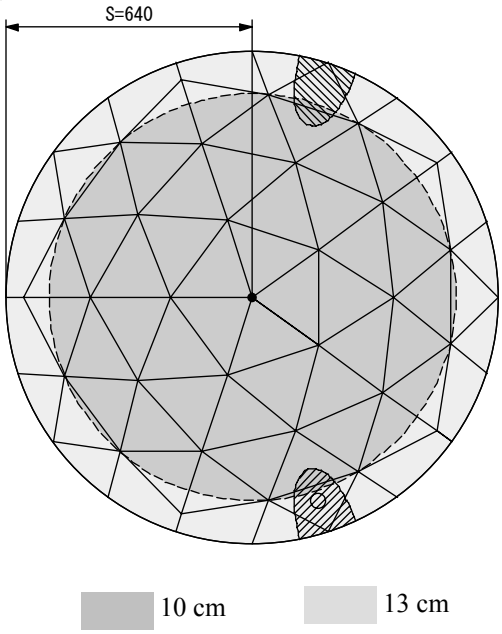

Fig. 7 Designed ice thickness

3.5 Pneumatic membrane for formwork

A P.V.C. membrane bag was placed on snow ground as shown in Fig. 10. This bag is fabricated by welding along the periphery after wrapping two pieces of plane sheet with 15 m diameter without 3 dimensional cutting, therefore the bag is easy to manufacture. The specifications of the P.V.C. membrane are as follows.

Weight: 4.3N/m^2, Thickness: 0.35mm, Tensile strength: longitudinal 588N/(3cm), traverse 549N/(3cm), Colour: orange

The weight of the bag is about 1.5 KN, therefore the bag is easy to carry by students themselves without machine. The cover ropes are laid on the membrane and connected to the end of the anchor rope. A portable air blower, which has a capacity of maximum airflow 40m^3/min. and maximum pressure 50mmAq, was used for the inflation. The inflation time was normally about 20 minutes. After the inflation, about 30 pieces of Styrofoam sticks for measuring the ice thickness under construction were set on the membrane.

Fig. 8 Manufacturing cover rope

Fig. 9 Construction of snow-ice foundation ring

Fig. 10 Set up membrane bag

Fig. 11 Air inflated membrane

Fig. 12 Application of snow and water

Fig. 13 Removing membrane

3.6 Application of snow and water

At the beginning stage, snow and water were carefully applied to the lower part of the membrane so as to make the zonal ice ring for transmitting smoothly forces between the periphery of the dome and the snow-ice foundation ring. After that, the snow was carefully blown onto the membrane by a rotary snow blower with the maximum throwing distance 17 m, and tap water was continuously sprayed on the thin snow layer by 4 adjustable nozzles with the maximum spraying distance of 15 m

and the spraying amount of 55 *l*/minute in total. The snow crushed with a snow blower is a type of sintering snow, with a high density and thickness per application of 0.4-0.5 g/cm^3 and 1 cm or less. The snow is blown at intervals of 60 to 90 minutes, with each application taking from 20 to 30 minutes, depending on the meteorological conditions. As the snow is being blown, water is continuously sprayed through an adjustable nozzle. The snow absorbs the sprayed water and keeps some of it from running down the sides. Since snow is a form of ice, it is natural that snow+water freezes faster than water alone; therefore, it is possible to complete a dome in less time and at higher temperatures by using snow in the construction. Experience shows that the thickness of the ice increases by about 1cm every 90 minutes when the outside temperature is approximately –10 ^{o}C, and its density is in the range of 0.83 to 0.88 g/cm^3. This ice has the favourable quality of limited

Fig. 14 Event 1 Rice cake making (Mochi-tsuki)

Fig. 15 Event 2 Piano concert

Fig. 16 Brilliant ice dome

cracking in the event of high-impact loading or rapid change in temperature. Fig. 12 shows a situation of the application of snow and water during construction, and the dome looked like a 'steaming giant bean-jam bun' when outside air temperature was below –13 ^{o}C.

3.7 Deflation

It takes 16 hours in total to complete the dome when the thickness at the apex is about 10 cm and 13 cm at the lower part as sown in Fig. 7. Just after the application of snow and water, the membrane was immediately deflated when it was early morning of January 14th, 2010. Fig. 13 shows the situation of removing the membrane after deflation.

3.8 Public event

After the construction, the students designed and produced the internal and external space of the dome. And they carried out the events by organizing student events in Evening of January 31, 2010. In the event, students explained the construction process of 15m ice dome in the ICE PANTHEON PROJECT 2010 and carried out the lighting presentation of lit candles around the dome, as shown in Fig. 16. We also enjoyed a piano concert and 'Rice cake making ('Mochi-tsuki' in Japanese)' inside of the dome.

4 Ending remarks

According to the shape and the creep deflection analysis of an axisymmetric ice dome based on membrane theory for a thin shell and invariant theory for the ice obeyed Glen's law during the creep, the non-spherical ice dome for Ice Pantheon Project improves significantly the structural performance compared to the conventional type of spherical dome. The dome is constructed by the method of blowing snow and spraying water on a pneumatic formwork consisting of a double-plane membrane bag and reticular cover rope. It can be constructed easily as long as there is equipment for spraying water, a snow blower, an air blower, a double-plane membrane bag, a reticular cover rope, snow, water and coldness. Also, the dome is environmentally compatible because it simply returns to the earth as water in spring. These factors have facilitated the application to winter structure in inland Hokkaido. This project shows the snow and coldness is a useful educational material for the students who study architecture and design subjects. Next winter, we have a plan to construct a larger 20 m span ice dome that has never been used for a practical structure before.

Acknowledgement

This project was supported by grant from 'Challenge Centre' of Tokai University. The authors thank the students for participating in Ice Pantheon Project 2010 of Tokai University.

References

[1] T. Kokawa. Ice Shell Construction for Winter Activity. *CD-ROM of International Symposium on New Perspective for Shell and Spatial Structures, IASS-APCS, Taipei, Taiwan,* 2003/10, 10 pp.

[2] Timoshenko,S. P. and Woinoesky-Krieger,S., 1959. Theory of Plates and Shells. McGraw-Hill, London, 2nd Ed., 436-447.

[3] Odqvist and Hult (translated by Sumio Murakami into Japanese, 1967). Theory of creep mechanics, Baihukan, 309pp.

[4] A. Assur. Some Promising Trends in Ice Mechanics. Physics and Mechanics of Ice, IUTAM SYMPOSIUM COPENHAGEN 1979 (Editor Per Tryde), 1-15.

[5] T. Kokawa, O. Itoh and T.Watanabe. Re-Challenge to 20-m Span Ice Dome. *CD-ROM of IASS in Nagoya* (Edited by Kunieda) 2001/10, TP187

[6] T. Kokawa. Field Study of a 30-m Span Ice-Dome, *Journal of IASS* Vol.43 (2002) n.2, August n.139, 93-100.